

## **Dy-doped CoNi Alloy Films Prepared by Electroplating Method**

*Yundan Yu\**, *Guoying Wei*, *Li Jiang*, *Hongliang Ge*

College of Materials Science and Engineering, China Jiliang University, Hang Zhou 310018, China

\*E-mail: [yuyundan@cjl.u.edu.cn](mailto:yuyundan@cjl.u.edu.cn)

*Received:* 16 September 2019 / *Accepted:* 12 November 2019 / *Published:* 31 December 2019

---

Dysprosium sulfate was added into the electrolyte to prepare CoNi alloy films by plating technology. The effect of dysprosium doping on electrochemistry process, composition, microstructure and corrosion resistance of CoNi was investigated. It was considered that CoNi alloy films electrodeposition was a kind of anomalous codeposition process. The percentage of cobalt content in CoNi films was higher than that of in the electrolyte. Higher concentration of dysprosium sulfate tended to decrease the cathodic polarization of CoNi electrodeposition resulting in the increase of deposition rate. The cobalt ions discharge was mainly affected by mass diffusion control. The rare earth dysprosium adsorbed on the cathode surface greatly affected the discharge process of cobalt ions to extremely decrease the content of cobalt in the CoNi alloy films. With the increase of dysprosium sulfate concentration in the electrolyte, the diffraction peak intensities of CoNi and cobalt decreased gradually while the surface morphology of CoNi alloy films changed from needle-like to nodular structure. Moreover, CoNi alloy films obtained in the electrolyte with higher dysprosium sulfate concentration possessed smaller grain size and condensed surface morphology that contributed directly to the improvement of anticorrosion performance.

---

**Keywords:** CoNi alloy films; dysprosium doping; anticorrosion performance

### **1. INTRODUCTION**

In recent years, with the rapid development of micromotor system, electronic components are gradually becoming miniaturized, intelligent and integrated. In the traditional motor industry, block magnet materials can basically meet the industrial application by appropriate processing. However, micromotor systems require micron-sized magnetic film materials, which are not easy to be cut from block magnets. The existing block magnets are usually brittle and can be cut in a limited size in industry, which cannot meet the requirement of the micromotor system. At present, nanometer or micron magnetic film materials are deposited directly on the surface of micromotor electronic components by physical and chemical methods to meet the needs of micromotor fields. Cobalt and nickel are elements with optimal ferromagnetic property. It is found out that CoNi alloy film has

wonderful magnetic and physical property which plays a big role in the field of micromotor systems. For example, Chen reported a kind of nanostructured CoNi thin films by plating technology. [1] Kim used electroless deposition method to prepare CoNi alloy thin films on silicon. [2] CoNi alloys with optimal structural and magnetic properties were obtained by Aubry reported in the journal of magnetism and magnetic materials. [3] Moreover, a kind of enhanced electronic and magnetic properties of electrodeposited amorphous cobalt-nickel nanosheets was fabricated by Yoon. [4] Although the CoNi film possesses optimal magnetic performance, the anticorrosion property is not good enough. Therefore, many non-metallic and oxide materials were doped into the CoNi thin films in order to greatly improve the anticorrosion performance. Yan and Liu designed a kind of NiCoP microcomposites with excellent wear and corrosion resistance. [5,6] SiO<sub>2</sub> was added in the electrolyte to electrodeposite NiCo-SiO<sub>2</sub> with excellent anticorrosion performance reported by Atuanya.[7] In addition, CoNiMnP thin films were obtained by magnetic plating technology to investigate their corrosion behaviors. [8] Except for particles like SiO<sub>2</sub>, P or Mn, it was found out that rare earth is also beneficial to extremely improve magnetic and corrosion resistance. Rare earth element has a special electronic layer structure, which is a strong internal adsorption element. After rare earth element is introduced into the solution, it could be preferentially adsorbed on the crystal defects on the catalytic metal surface to change the microstructures and refine the grains of thin films.[9-14] The mechanism associated with the effect of rare earth on magnetic and chemical properties has not been widely reported so far. Therefore, in the paper, dysprosium was added in the bath to electrodeposite CoNi alloy film by plating technology. Influences of dysprosium on composition, microstructure, surface morphology and anticorrosion of CoNi thin films were studied.

## 2. EXPERIMENTAL

CoNi thin films were prepared by plating technology from the acid bath with different concentrations of dysprosium sulfate. The detail information about plating parameters was listed in Table 1.

**Table 1.** Solution formula and plating parameters of CoNi alloy films

Chemical agents and technology parameters	Value
NiSO <sub>4</sub> ·7H <sub>2</sub> O	30 g/L
CoSO <sub>4</sub> ·7H <sub>2</sub> O	15 g/L
H <sub>3</sub> BO <sub>3</sub>	30 g/L
Na <sub>2</sub> SO <sub>4</sub>	20 g/L
Dy <sub>2</sub> (SO <sub>4</sub> ) <sub>3</sub> ·8H <sub>2</sub> O	0~0.4 g/L
<i>J</i> (current density)	1.5 Adm <sup>-2</sup>
pH	6
<i>T</i>	333 K
<i>t</i> (plating time)	1800 s

According to the plating parameters of table 1, two main salts including NiSO<sub>4</sub> and CoSO<sub>4</sub> were selected to offer Ni<sup>2+</sup> and Co<sup>2+</sup> during the electrodeposition process. Na<sub>2</sub>SO<sub>4</sub> was considered as the conductivity salt in the system while H<sub>3</sub>BO<sub>3</sub> was chosen as the buffer agent to adjust the pH value near cathode during the plating process. Dy<sub>2</sub>(SO<sub>4</sub>)<sub>3</sub> ranged from 0~0.4 g/L was added in the electrolyte to investigate their effects on electrodeposition process of CoNi thin films. The plating system of CoNi thin films was based on three electrodes. Meanwhile, pure copper sheet with 2×2 cm<sup>2</sup> size was working electrode while pure platinum sheet of 3×3 cm<sup>2</sup> was chosen as counter electrode. Saturated calomel electrode (SCE) was used as the reference electrode. Firstly, the pure copper sheet was polished by a polish machine. And then, an alkaline solution (12 g/L NaOH) and an acid solution (10% HCl) were used to get rid of the oils and oxides on the copper surface respectively. Finally, the substrate was put into 100 ml plating bath to perform electrodeposition for 1800 s. The composition of CoNi alloy films was analyzed by energy dispersive spectrometer (EDX1800B) with 20 kV. Scanning electron microscope (TM3000) was selected to observe the surface morphology of samples. Microstructure of the samples was carried out using an X-ray diffraction (XPert Philips PW1830) with 1°/min scanning rate, which used a Cu K $\alpha$  radiation as an incident beam and worked at 40 kV, 150 mA. Electrochemistry analysis, such as polarization and cyclic voltammetry curves were analyzed by electrochemistry station (Parstat 2273) combined with quartz crystal microbalance. The scanning potential range of polarization curve is from -0.75 V to -0.45 V with 1 mV/s scanning rate at 3.5% NaCl solution. The scanning rate of cyclic voltammetry curve is 20 mV/s.

### 3. RESULT AND DISCUSSION

#### 3.1 Cyclic voltammetry curves of CoNi alloys

Cyclic voltammetry curves of Co, Ni, CoNi and Dy-CoNi carried out on quartz crystal microbalance were used to analyze the oxidation and reduction process of CoNi. As seen from figure 1, anodic oxidation peak are apparently observed in the curves and no obvious cathodic reduction peaks are detected among the potential regions. Oxidation current of cobalt is much higher than that of nickel. That is because anticorrosion performance of nickel is much better than cobalt. The self-corrosion potential of nickel is more positive than cobalt. The oxidation currents of CoNi alloys are composed of the current contributions of oxidation of Co and Ni. Moreover, according to figure 1(a), the deposition potential of Co, Ni and CoNi is equal to -0.78 V, -0.81 V and -0.76 V respectively which is consistent with the works reported by others.[15-17] It can be found out that the deposition potential of the CoNi alloy is more positive than Co and Ni. Compared with CoNi cyclic voltammetry curves with and without dysprosium, it is conspicuous that the rare earth can greatly decrease cathode polarization which is beneficial to activate cathode behavior resulting in the acceleration of electrodeposition process. As a kind of rare elements, dysprosium has a special electronic layer structure which can be preferentially adsorbed on the crystal defects on the catalytic metal surface to reduce surface energy and improve the nucleation rate. Moreover, due to the low electronegativity of dysprosium, some parts of dysprosium appear as positive ions, which act as catalysts to accelerate the reduction of metal ions.[18-21] As shown in figure 1(b), the CoNi thin film deposited from the bath with dysprosium sulfate possesses more deposition mass than others.

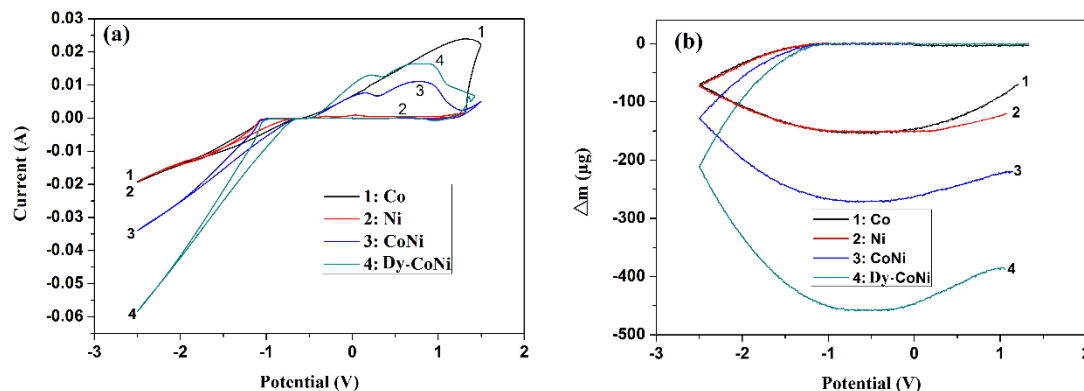


**Figure 1.** (a) Cyclic voltammetry curves of 0.05 M Co, 0.05 M Ni, 0.05 M CoNi and Dy-CoNi (0.05 M CoNi and 0.1 g/L dysprosium sulfate) with 20 mV/s scan rate; (b) the mass changing detected by quartz crystal microbalance;

### 3.2 Composition and microstructure of CoNi alloys

In order to study the effect of rare earth dysprosium on the composition of CoNi films, EDX was used to analyze the composition. As seen from figure 2, the relationship between the concentrations of dysprosium sulfate and films composition is revealed. It is clearly found that, as the concentration of dysprosium sulfate varying from 0.1 g/L to 0.4 g/L, the content of cobalt decreases from 81% to 46% while the amounts of nickel increases from 19% to 54%.

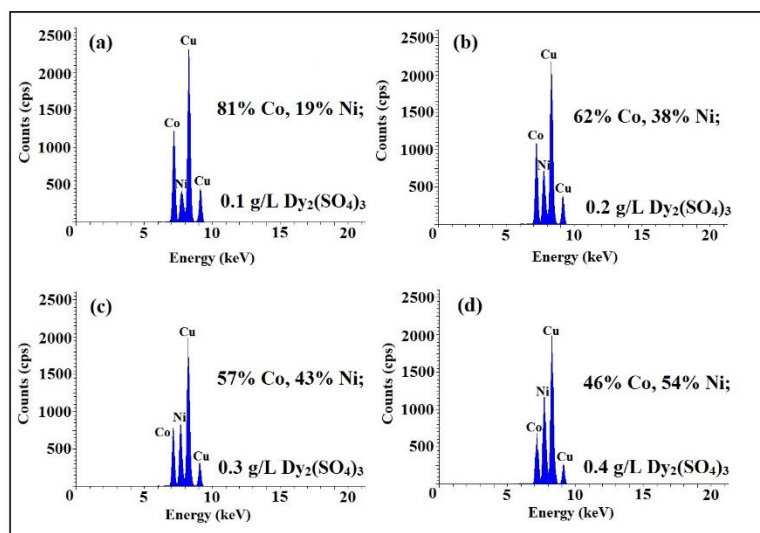
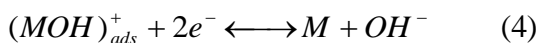
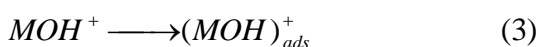
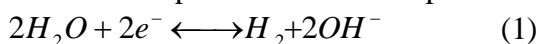


**Figure 2.** Composition of CoNi films electrodeposited from baths with different concentrations of dysprosium sulfate

There is no dysprosium element found in the EDX patterns. Maybe the amount of dysprosium is too few to be detected by the equipment. The deposition potential of dysprosium is more negative than -2.4 V, so it is difficult to electrodeposit from the aqueous directly. However, higher

concentration of dysprosium sulfate could help to increase nickel content, but decrease cobalt content in CoNi alloy films. It is known that the discharge process of  $\text{Co}^{2+}$  is mainly affected by mass transfer while  $\text{Ni}^{2+}$  discharge is mainly caused by activation control.[22] Therefore, compared with discharge process of nickel, the adsorption film formed on the cathode surface caused by rare earth can obviously affect the discharge process of cobalt to inhibit cobalt deposition and reduce amounts of cobalt in the films. The more dysprosium sulfate are added in the bath, the greater the hindrance to cobalt deposition.

It was noticed that electrodeposition process of CoNi was considered as a kind of typical anomalous codeposition phenomenon. According to the theory, the standard deposition potential of nickel was more positive than cobalt. Nickel was easier to be electrodeposited than cobalt. However, according to the EDX patterns, it was found out that cobalt content in the CoNi films was always higher than that of in the electrolyte. This phenomenon was considered as anomalous codeposition, which was reported mainly in codeposition of iron group metals. The hydroxide suppression mechanism was accepted as a kind of explanations about anomalous codeposition.[23-25]



During the electrodeposition process, metal ions and hydrogen ions are extremely consumed near the cathode that attributed directly to the increase of pH values resulting in the formation of hydroxide colloid. According to the equations, M represents Ni and Co atoms. It is believed that, compared with hydroxide colloid of nickel, both the  $\text{Co}(\text{OH})^+$  and  $\text{Co}(\text{OH})_2$  are favor to be adsorbed on the surface of cathode which restrain the transportation and reduction process of nickel ions resulting in the decline of nickel contents in the CoNi films. Generally speaking, the anomalous codeposition is caused by the competitive adsorption of  $\text{M}(\text{OH})_2$  and  $(\text{MOH})^+$  during the electrodeposition.

XRD patterns of CoNi films obtained from the baths containing various concentrations of dysprosium sulfates are shown in figure 3. Four typical CoNi diffraction peaks of CoNi(111), CoNi(200), CoNi(220) and CoNi(311) are observed at  $2\theta=44.5^\circ$ ,  $2\theta=51.8^\circ$ ,  $2\theta=76.4^\circ$  and  $2\theta=93.1^\circ$  respectively. The diffraction intensities of CoNi samples are strong and obvious indicating better crystal structures. This result of CoNi structure was reported by many researchers.[26-27] Moreover, peaks of cobalt with hcp structures could also be observed in the XRD patterns. Along with the increase of dysprosium sulfate concentration, diffraction intensities of CoNi sample and hcp-cobalt peaks decrease extremely. Higher concentration of dysprosium sulfate intends to decrease the cobalt content in the CoNi films which contributes directly to the decrease of diffraction intensity associated with cobalt. In the electrodeposition process of CoNi alloy films, adsorption characteristics caused by dysprosium doping changes the structure of interface double layer. The electrodeposition and interfacial diffusion of metal ions are affected, so that the metal atoms cannot reach the normal lattice junction point which result in the changing of microstructures. After the addition of rare earth, it is preferentially adsorbed on the active point of crystal growth, so as to effectively inhibit the growth of crystals and refine the grain size that attributes to the decrease of crystalline and diffraction intensity.

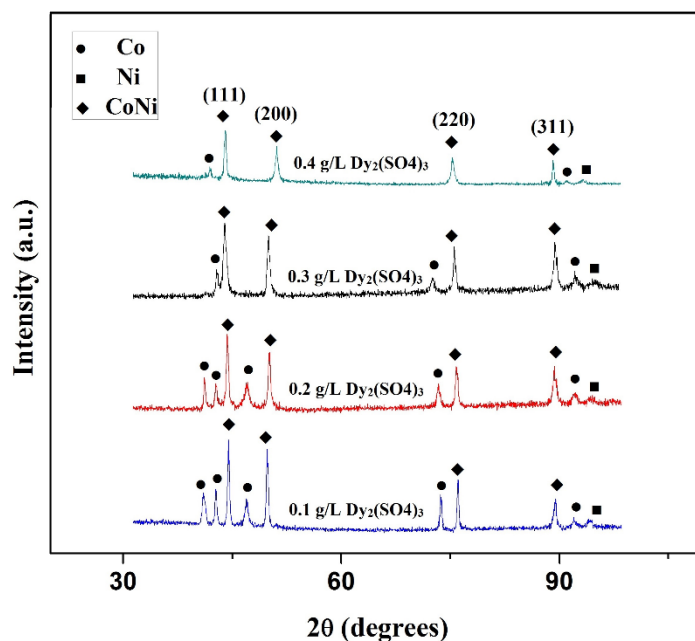


**Figure 3.** XRD patterns of CoNi films electrodeposited from baths with different concentrations of dysprosium sulfates

### 3.3 Surface morphology and anticorrosion of CoNi alloys

Surface morphologies of CoNi alloy films electrodeposited from baths with different concentrations of dysprosium sulfates are shown in figure 4.

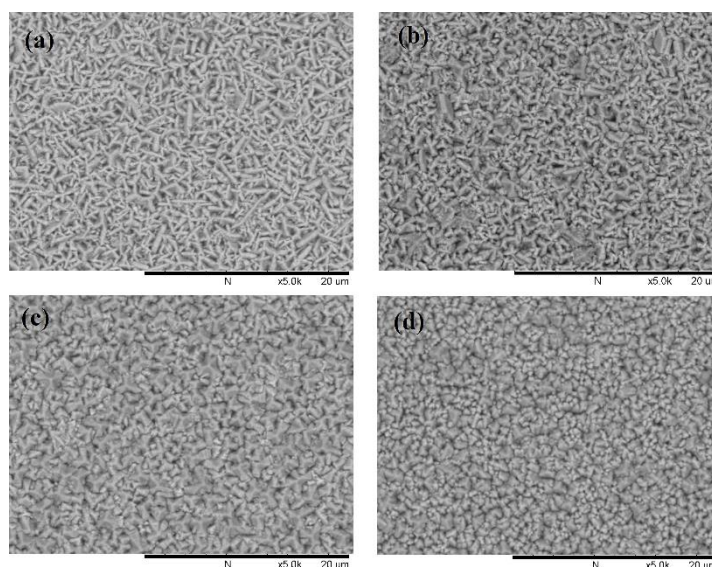


**Figure 4.** Surface morphology of CoNi alloy films (a) 0.1 g/L  $\text{Dy}_2(\text{SO}_4)_3$ ; (b) 0.2 g/L  $\text{Dy}_2(\text{SO}_4)_3$ ; (c) 0.3 g/L  $\text{Dy}_2(\text{SO}_4)_3$ ; (d) 0.4 g/L  $\text{Dy}_2(\text{SO}_4)_3$ ;

As seen from SEM images, the surface morphologies of CoNi films are totally different. CoNi

films obtained from the bath with 0.1 g/L dysprosium sulfate possess needle-like structures. Regarding to the XRD patterns, cobalt with hcp structures is precipitated in large quantities on the metal surface leading to needle-like structures. It is found out that, the higher the cobalt with hcp structures precipitation, the more obvious the acicular structures. With the amount of dysprosium sulfate increases, the surface morphology of CoNi films transfers from needle-like to typical nodular structures. Higher concentrations of dysprosium sulfate tend to decrease the cobalt content in the films and refine the grain size leading to the change of surface morphology.

Polarization curves carried out by electrochemistry station (PARSTAT 2273) were used to evaluate the anticorrosion performance of CoNi alloy films obtained from baths with different concentrations of dysprosium sulfates. The polarization experiment was based on three electrodes system. Meanwhile, the CoNi film ( $1 \times 1 \text{ cm}^2$ ) and platinum sheet ( $2 \times 2 \text{ cm}^2$ ) were chosen as the working and counter electrode respectively. Saturated calomel electrode was chosen as the reference electrode. The scanning rate was 1 mV/s. The corrosion current and voltage were calculated based on the intersection gotten from the tangents of anodic and cathodic polarization curves. Table 2 listed the self corrosion potential and corrosion current of CoNi films based on figure 5.

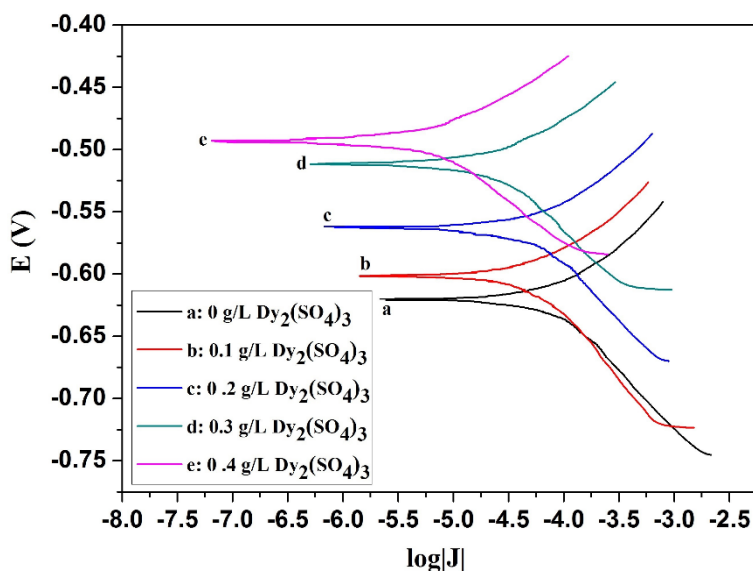


**Figure 5.** Polarization curves of CoNi films in 5 % NaCl solution

**Table 2.** Corrosion potential and current of CoNi alloy films

Dy <sub>2</sub> (SO <sub>4</sub> ) <sub>3</sub> (g/L)	Percentage of Co and Ni	Corrosion Potential(V <sub>SCE</sub> )	Corrosion Current (μAcm <sup>-2</sup> )
0	87 %, 13 %	-0.621	-50.17
0.1	81 %, 19 %	-0.601	-25.12
0.2	62 %, 38 %	-0.563	-16.59
0.3	57 %, 43 %	-0.512	-7.58
0.4	46 %, 54 %	-0.493	-2.82

Along with the increase of dysprosium sulfate concentration, amounts of nickel in CoNi films increase simultaneously that contribute to more positive corrosion potential. Moreover, the CoNi film fabricated from the electrolyte with 0.4 g/L dysprosium sulfate possess the smallest corrosion current and optimal anticorrosion performance due to the compact surface with smaller nodular particles. The dysprosium adsorbed on the active point of crystal growth can effectively inhibit the growth of crystals and refine grain size to form films with denser surface resulting in the improvement of corrosion resistance performance.

#### 4. CONCLUSION

CoNi alloy films were obtained from the baths with different concentrations of dysprosium sulfate. Influences of dysprosium on cyclic voltammetry, composition, microstructure, surface morphology and corrosion resistance of CoNi alloy films were investigated. It was found out that dysprosium could greatly decrease cathode polarization during CoNi plating process which was beneficial to activate cathode behavior resulting in the acceleration of electrodeposition process. Higher concentration of dysprosium sulfate could help to increase nickel content, but decrease cobalt content in the CoNi alloy films. The dysprosium adsorbed on the active point of crystal growth can effectively inhibit the growth of crystals and refine grain size to change the microstructures of CoNi films. With the increase of dysprosium sulfate concentration, the microstructures of CoNi films change from acicular to typical nodular structures. The CoNi film fabricated from the electrolyte with 0.4 g/L dysprosium sulfate possess the smallest corrosion current and optimal anticorrosion performance due to the compact surface with smaller and denser nodular particles.

#### ACKNOWLEDGEMENT

This paper is supported by Science and technology plan projects of Zhejiang province (2018C37043), National Natural Science Foundation (No. 51771776) and Open project of key laboratory (2018K05).

#### References

1. Q.S. Chen, Z.Y. Zhou and G.C. Guo, *Electrochim. Acta*, 113 (2013) 694.
2. D.U. Kim, R. Shanmugam and M.R. Choi, *Electrochim. Acta*, 75 (2012) 42.
3. E. Aubry, T. Liu and A. Bilard, *J. Magn. Magn. Mater.*, 422 (2017) 391.
4. S. Yoon, J.Y. Yun and J.H. Li, *J. Alloys Compd.*, 693 (2017) 964.
5. Y.H. Yan and Y.P. Tian, *Mater. Des.*, 111 (2016) 230.
6. C.S. Liu and F.H. Su, *Trans. Met. Soc. China.*, 28 (2018) 2489.
7. C.U. Atuanya and D.I. Ekweghiariri, *Def. Technol.*, 14 (2018) 64.
8. Y.D. Yu and G.Y. Wei, *Surf. Eng.*, 33 (2017) 483.
9. X.M. Zheng, P.Y. Zhang and S. Tao, *Thin Solid Film*, 638 (2017) 400.
10. H. Wang, R. Liu and K. Chen, *Thin Solid Film*, 519 (2011) 6438.
11. L.L. Wang and L.M. Tang, *Surf. Coat. Technol.*, 192 (2005) 208.
12. G. Jin and B.W. Lu, *J. Rare Earth.*, 34 (2016) 336.
13. S. Ghosh and R. Ganesan, *J. Nucl. Mater.*, 467 (2015) 280.

14. J.T. Kong and S.Y. Shi, *Electrochim. Acta*, 53 (2007) 2048.
15. P. Cojocaru, L. Magagnin, E. Gomez and E. Valles, *J. Alloys Compd.*, 503 (2010) 454.
16. P. Cojocaru, M. Spreafico, E. Gomez, E. Valles and L. Magagnin, *Surf. Coat. Technol.*, 205 (2010) 195.
17. Y.D. Yu, G.Y. Wei, H.L. Ge, L. Jiang and L.X. Sun, *J. Magn.*, 22 (2017) 2233.
18. Y. Gao and W.L. Chen, *Rare Metal Mater. Eng.*, 46 (2017) 2070.
19. H.A. Sorkhabi and M.M. Haghghi, *Surf. Coat. Technol.*, 202 (2008) 1615.
20. Q. Zhang, Y.X. Hua, C.Y. Xu and P. Dong, *J. Rare Earths*, 33 (2015) 1017.
21. E. Bourbos, I. Giannopoulou and A. Karantonis, *Rare Earths Ind.*, 13 (2016) 199.
22. D. Choudhuri and S.G. Srinivasan, *Comput. Mater. Sci.*, 159 (2019) 235.
23. H. Hu and L.P. Liu, *J. Alloy Compd.*, 715 (2017) 384.
24. D.M. Dryden and T. Sun, *Electrochim. Acta*, 220 (2016) 595.
25. M.A.K. Mortaga, *Appl. Surf. Sci.*, 252 (2005) 1035.
26. S. Pane, E. Gomez, J.G. Amoros, D. Velasco and E. Valles, *Appl. Surf. Sci.*, 253 (2006) 2964.
27. S. Pane, E. Gomez, J.G. Amoros, D. Velasco and E. Valles, *J. Electroanal. Chem.*, 604 (2007) 41.

© 2020 The Authors. Published by ESG ([www.electrochemsci.org](http://www.electrochemsci.org)). This article is an open access article distributed under the terms and conditions of the Creative Commons Attribution license (<http://creativecommons.org/licenses/by/4.0/>).